AGU PUBLICATIONS

Geophysical Research Letters

RESEARCH LETTER
10.1002/2016GL070042

Key Points:
- In the WCSB, the probability that hydraulic fracturing may induce events of $M \geq 3$ is 0.010 to 0.026 at the 95th percentile confidence limit
- The proximity of a nearby disposal well increases the likelihood that hydraulic fracture operations will be associated with seismicity
- Proximity to the Swan Hills Formation is associated with increased seismogenic potential of hydraulic fracture operations

Supporting Information:
- Supporting Information S1

Correspondence to:
H. Ghofrani,
hghofra@uwo.ca

Citation:
Ghofrani, H., and G. M. Atkinson (2016), A preliminary statistical model for hydraulic fracture-induced seismicity in the Western Canada Sedimentary Basin, *Geophys. Res. Lett.*, *43*, 10,164–10,172, doi:10.1002/2016GL070042.

Received 14 JUN 2016
Accepted 22 SEP 2016
Accepted article online 23 SEP 2016
Published online 9 OCT 2016

A preliminary statistical model for hydraulic fracture-induced seismicity in the Western Canada Sedimentary Basin

Hadi Ghofrani[1] and Gail M. Atkinson[1]

[1]Department of Earth Sciences, Western University, London, Ontario, Canada

Abstract We characterize the statistical relationship between hydraulic fracturing and seismicity in western Canada by using the concept of cellular seismicity. We determine the regionally averaged probability that hydraulic fracture operations will be associated with $M \geq 3$ seismicity within a 10 km grid cell. This rate is 0.01 to 0.026 at the 95th percentile confidence limit. Monte Carlo simulations confirm that the observed correlations are extremely unlikely (≪1%) to have been obtained by chance. Proximity to a disposal well and proximity to the Swan Hills Formation, which has been suggested as a proxy for basement controlled faults, appear to increase the likelihood that hydraulic fracturing will trigger seismicity.

1. Introduction

In many parts of North America that have been historically quiet seismically, the rate of earthquakes of moment magnitude (M) ≥3 has increased significantly over the last decade [*Ellsworth*, 2013; *Atkinson et al.*, 2016]. In the central U.S., most induced seismicity is linked to deep disposal of coproduced wastewater from oil and gas extraction [*Ellsworth*, 2013; *Karenen et al.*, 2014; *Frohlich et al.*, 2014; *Rubinstein and Babaie Mahani*, 2015; *Weingarten et al.*, 2015; *Hornbach et al.*, 2015]. By contrast, in the Western Canada Sedimentary Basin (WCSB) most recent cases of induced seismicity are highly correlated in time and space with hydraulic fracturing, wherein fluids are injected under high pressure during well completion to induce localized fracturing of rock [*B.C. Oil and Gas Commission*, 2012, 2014; *Rubinstein and Babaie Mahani*, 2015; *Atkinson et al.*, 2015a; *Farahbod et al.*, 2015; *Schultz et al.*, 2015a, 2015c; *Atkinson et al.*, 2016]. In the central U.S., some of the larger events, in particular the 2011 *M*5.7 Prague, Oklahoma, earthquake, have caused significant damage [*Choi*, 2012; *Ellsworth*, 2013], leading to concern that such activities in the proximity of critical facilities or vulnerable infrastructure may pose an unacceptable increase in seismic risk [*Taylor et al.*, 2015].

The relationship between energy operations and induced seismicity is complex and will be specific to an area. At present, there is no physical model that can predict whether seismicity will occur for a particular set of parameters, and in fact, many of the parameters that would be required to develop such a model are currently unknown [*National Research Council*, 2013]. Consequently, models of induced seismicity hazards are largely statistical in nature, typically relying on empirical analyses of the observed rate and spatial distribution of induced events above a certain magnitude [*Atkinson et al.*, 2015b; *Weingarten et al.*, 2015].

In this study, we develop a preliminary statistical model of the likelihood that horizontally fractured wells (HF wells) in the WCSB will trigger earthquakes of $M \geq 3$ and map how that likelihood varies spatially. Our aim is to facilitate the forecasting of induced seismicity potential for future HF operations. This differs from an exercise aimed at identifying individual wells that initiated past sequences. For future operations, we are interested in the probability that a significant sequence of events may be triggered (the activation probability). The rate of seismicity in a probabilistic seismic hazard analysis (PSHA) for induced seismicity is the product of the activation probability and the conditional earthquake rate (conditioned on activation). Thus, changing the activation probability is equivalent to changing the seismicity rate parameter (Gutenberg-Richter *a* value), which significantly impacts the expected ground motions [*Atkinson et al.*, 2015a, 2015b].

2. Data and Methods

The database used in this study is an updated version of that of *Atkinson et al.* [2016]. Seismicity data were obtained for the time period from 1985 to 31 August 2015 (www.inducedseismicity.ca). All magnitudes are moment magnitude (M). We selected the $M \geq 3$ level as the threshold magnitude level for the analysis because the catalogue is considered to be relatively complete above this level since 1985 [*Adams and Halchuk*, 2003]. Moreover, $M \geq 3$ represents a significant level of ground shaking, likely to be felt at close distances [*Atkinson et al.*, 2014]. There are 14,046 HF wells (i.e., lateral wells stimulated with multistage hydraulic fracture treatments) that lie within the WSCB study area. A map of the database of seismicity and wells used in the analysis is provided in the supporting information.

We subdivide the study region into small cells and evaluate for each cell whether there is a relationship between seismicity and hydraulic fracturing. The rationale for dividing the region into cells is to be able to evaluate susceptibility to seismicity in spatially discrete areas, rather than looking at individual wells. Such an approach is more useful for hazard forecasting in specific areas. We cover the entire study region with an overlapping grid of points having a uniform 10 km spacing (Figure 1). At each grid point we define a cell as the circular area within a 10 km radius of the point. Ten kilometer is a suitable grid interval for the study for two reasons: (i) this is the approximate location uncertainty of earthquakes in many parts of the study area, and thus, events listed in the catalogue as being within 10 km of an HF well may actually be located within only meters of the well, and (ii) 10 km is the distance interval of most practical concern for induced seismicity, as the motions from moderate events can be strong at very close distances, but may not produce strong shaking at larger distances [*Atkinson*, 2015].

Every cell that contains at least one HF well is classed as "active," while the remainder of cells are classed as "null." We considered that a temporal correlation may exist between seismicity and HF wells if an event ($M \geq 3$) occurred within a window beginning with the commencement of hydraulic fracturing and ending 3 months after the completion of treatment. This time window was selected based on reported time lags for a representative subset of our study area [*Farahbod et al.*, 2015]. If an active cell contains at least one event that meets the temporal criterion for correlation, then its grid point is a "hit" for potential induced seismicity. Miss cells are active cells that are not classified as a hit. The total number of hit points (N_{Hit}) and the total number of active cells (N_{Active}) can be used to calculate the ratio $R_{h10} = N_{\mathrm{Hit}}/N_{\mathrm{Active}}$, which is an estimate of the regionally averaged probability that operations in a 10 km radius cell may be associated with seismicity. We consider that the quantity R_{hA} is a rough estimate of the prior probability of inducing seismicity by commencing HF operations in a small area in the WCSB in a Bayesian sense; note that the area in this case is that associated with a circle of the given radius (i.e., an area of $\pi(10\ \mathrm{km})^2 = 314\ \mathrm{km}^2$).

3. Results

The active and hit cells are shown in Figure 1. There are 4523 cells, of which 1825 cells are "active" and 2698 cells (=total active) are null**.** Of the active cells, 67 are classified as hits**.** Therefore, the regionally averaged cellular hit rate is $R_{h10} = N_{\mathrm{Hit}}/N_{\mathrm{Active}} = 67/1825 = 0.0367 \sim 0.04$. Note that the cells we detect as hits agree well with those determined to be associated with HF wells from more detailed site-specific studies (as shown in Figure S1 in the supporting information). This provides confidence that the simple screening methodology is reliably identifying cells having associated events.

We have not attempted to definitively classify the causation of the correlation between oil and gas operations and seismicity on an cell-by-cell basis, due to lack of specific information in the public databases. However, we devise a probabilistic metric, the discrimination ration (DR) to show the confidence of the association in each hit cell. In brief, the discrimination ratio is the ratio obtained by dividing the fraction of events meeting the HF criterion by the fraction of time that was covered by HF windows. In Figure 1, we use this concept to illustrate the confidence in the association of seismicity with hydraulic fracturing and disposal (additional details provided in the supporting information).

To investigate whether the observed correlation could be obtained by random chance, we perform a Monte Carlo analysis. We consider the study area (Figure 1) as an areal source zone in the context of a classic PSHA. The zone has the observed rate of 270 earthquakes of $M \geq 3$ in the study period (1985–2015). We use the Monte Carlo earthquake simulation algorithm EQHAZ1 [*Assatourians and Atkinson*, 2013] to simulate 1500 earthquake catalogues for the study area and time period, each of which has 270 events of $M \geq 3$, distributed randomly in time and space, in which seismicity is assumed to be a Poisson process. (Note that the results are not sensitive to the assumed maximum magnitude and *b* value, as we are only interested in the total number of events above $M = 3$.)

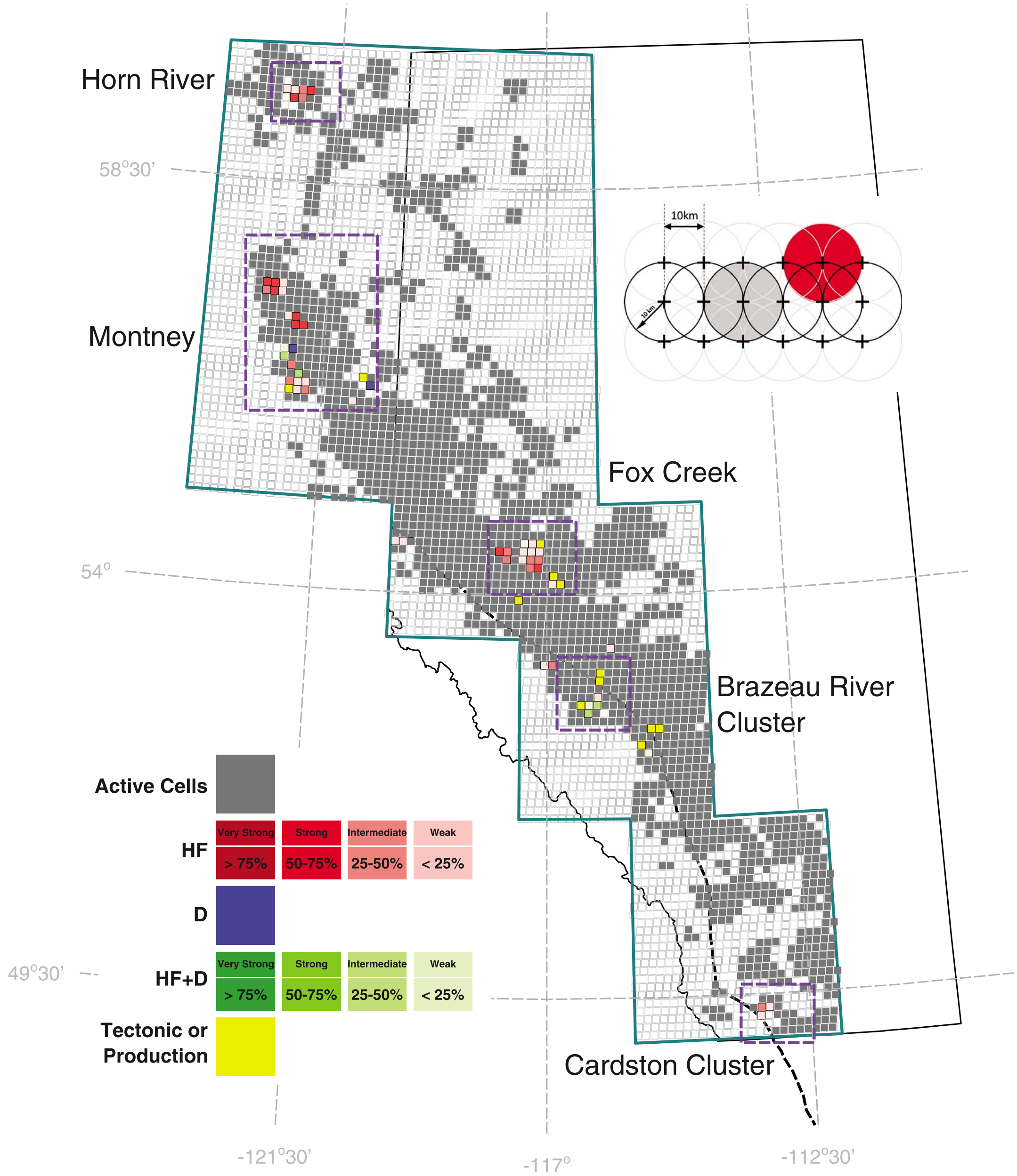

Figure 1. Pattern of active HF wells (dark gray cells) in WCSB. The purple rectangles identify areas where seismicity has been previously attributed to oil and gas operations. Shading in this figure is based on rectangles for graphical reasons, but the actual cells are circular in shape, and have a 10 km radius; see inset for enlargement of the actual geometry. The likelihood of seismicity in hit cells being associated with either hydraulic fracturing, or the combination of HF and disposal, as determined in this study, is indicated by shading.

3.1. Randomly Distributed Events

If we assume that earthquakes are randomly distributed in both time and space, then the maximum number of hit cells that we obtain in 1500 trials is 47. By contrast, we had 67 hits in the observed data set. This degree of spatiotemporal correlation between earthquakes and the portfolio of HF well operations was observed 0 times in 1500 independent simulations of the regional seismicity pattern. In the 1500 random trials, the median hit rate was 21 cells, with the 5th to 95th percentile rates spanning the range from 11/1825 to 33/1825. Thus, we are 95% confident that at least 34(=67–33) cells are actually hits (i.e., above and beyond those expected by random chance). The hit rate at the 95th confidence percentile is N_{Hit} at 95%CI/$N_{\mathrm{Active}} = 34/1825 \approx 0.02$, and at the 5th percentile it is 56(=67–11)/1825 ≈ 0.03.

3.2. Clustered Analysis: Smoothed Seismicity

It could be argued that it is unreasonable to treat the seismicity in the study area as randomly distributed in space, when it is so clearly clustered. If we assume that the clustering is natural, due to tectonic factors that favor seismicity in some areas, then we need to account for this in our analysis of the likelihood that hydraulic fracturing is inducing the seismicity. It could be that hydraulic fracturing just happens to coincide with areas that are prone to seismicity.

To address this possibility, the smoothed seismicity option is used in EQHAZ1, which follows the *Frankel* [1995] methodology in clustering the likelihood of the synthetic events in space, according to their observed clustering in the catalog. In this exercise, the observed number of $M \geq 3$ events was distributed randomly in time following a Poisson distribution, but clustered in space as in the observed catalogue. Thus, only the timing of the events with respect to HF well operations is considered to be random. The degree of correlation with the portfolio of active cells was observed 2 times in 1500 trials. The 95th percentile of the number of hit cells is 48, while the 5th percentile is 20. Thus, we are 95% confident that at least 19(=67–48) cells are actually hits. The hit rate at the 95th percentile is: N_{Hit} at 95%CI/N_{Active} = 19/1825 = 0.0104.

4. Other Possible Causes of the Correlation

The analysis shows that seismicity and HF operations have a high degree of correlation. Even if we use the smoothed seismicity approach to build the observed spatial clustering within the catalogue into the analysis, the occurrence rate of events in a short time window following HF treatments is too high to be coincidental. However, it may be possible that other factors are also at play. The most likely of these is that disposal wells may be partly or largely responsible for the events. Perhaps increased HF operations lead to volumes of fluid that are then disposed of in nearby wells (within days to weeks), triggering the seismicity.

To investigate the role of disposal wells, we identified all disposal wells within each of the 67 hit cells and considered additional criteria to quantify the likelihood that the disposal wells were involved in triggering the seismicity. These additional tests are described in the supporting information.

Figures S3–S35 show how each hit cell was classified as HF, disposal (referred to as "D"), HF + D, or other. The additional screening identified disposal wells as being a contributing cause of the associated seismicity in 10 cells. Of these, two cells are flagged as D and eight cells are flagged as HF + D. We retain 18 cells in which the seismicity is associated with HF wells but not disposal wells. There are eight active cells for which the DR falls below the 75th percentile, and for which no disposal well is nearby. For these cells the seismicity is likely to be tectonic or might be production-related. Production-related seismicity is suspected if there was no historical seismicity in the area prior to oil and gas activity, but yet there is no association with either HF wells or disposal wells due to missing operational information. In conclusion, we find that of 67 active cells in which HF operations occurred, 44 cells have $M \geq 3$ seismicity associated with HF wells, 8 cells have seismicity that is associated with the combination of HF and disposal, 2 cells are associated with production, 2 cells are associated with disposal, and 11 cells have a tectonic association.

5. Sensitivity Analysis

In the foregoing analysis we considered any earthquake within a circular grid with a radius of 10 km to be associated with a well in the same grid if the event happened within a specified time window. This distance of association is motivated by the average uncertainty error of 10 km in epicentral locations in the WCSB [*Schultz et al.*, 2015b]. The temporal criterion of 3 months following HF operations was designed to consider the possible delay time for migration of a pressure front through the diffusion of pore pressure [*Farahbod et al.*, 2015]. It could be argued that either or both of these filters are too liberal, because multistage HF operations are sequential treatments with a very concentrated effective area limited to the vicinity of the well. The pressurization during hydraulic fracturing affects only limited volumes of rock, typically several hundred meters in extent, and pressurization typically lasts only a few hours [*Zoback*, 2012]. To analyze the sensitivity of our results to these filtering parameters, we also tested our analysis using alternative spatial association distance and temporal criterion. Moreover, we also examined sensitivity of results to issues such as whether one considers overlapping or nonoverlapping cells and what shape of cells is used (circular, rectangular, or hexagonal). For brevity, we do not provide all of these results here, but we concluded that the results are insensitive to grid shape and overlap, but show some sensitivity to grid radius and the time window considered, as elaborated in the following.

5.1. Grid Radius (Spatial Sensitivity)

To analyze the sensitivity of our results to the spatial filtering parameter, we repeated our analysis by using a spatial association distance of 5 km (instead of 10 km). We note that any events that occurred near an HF operation, but which were mislocated by more than 5 km, would be missed in this exercise.

For this test, we find 51 hit cells associated with earthquakes in the WCSB after filtering, compared to 67 hit cells obtained with a 10 km radius. We also have more active cells, because the use of overlapping windows causes the number of active cells to increase from 1825 (10 km cell radius) to 4366 (5 km cell radius). Thus, the hit rate considering circular cells with a 5 km radius is significantly smaller at $R_{h5} = 51/4366 = 0.012$.

However, the significance of the observed rate also changes. If we repeat the Monte Carlo analyses to find the likelihood that this result could be obtained by random chance, we find that the 5th to 95th percentile range of the hit rate is 2 to 15 (i.e., $2/4366 = 0.00046$ to $15/4366 = 0.0034$) if we consider seismicity to be randomly distributed in space. If we use the smoothed seismicity option to consider clustering, the corresponding range of the hit rate is 5 to 22 (i.e., $5/4366 = 0.0011$ to $22/4366 = 0.0050$). Thus, a smaller grid size does not change the essential conclusion that the association with HF operations is highly significant and very unlikely to occur by chance.

5.2. HF Window (Temporal Sensitivity)

We also checked the sensitivity of results to the adopted HF window length. Instead of using a 3 month time window after the date of the HF treatment, we searched for possible associated events in a narrower window of 1 month. For this configuration, we find 52 hit cells (instead of 67) from 1825 active cells. The corresponding hit rate is $R_{h10} = 52/1825 \approx 0.03$, with the 5th to 95th rate by random chance lying between 4 and 19 ($19/1825 \approx 0.01$ to $4/1825 = 0.0022$), for the uniform seismicity option. For the smoothed seismicity option, the corresponding range of the 5th to 95th percentile range of the hit rate expected by chance is higher, 9 to 28 ($28/1825 = 0.015$ to $9/1825 = 0.0011$). We conclude that there is some sensitivity to the window length, but the association between seismicity and HF operations is still highly significant. This points to the importance of further studies to determine the time scale over which the pore pressure signature of HF operations may persist.

6. Discussion

The recent earthquake rate changes in WCSB are highly correlated with HF wells, in a way that is highly unlikely to be coincidental. It is apparent that in some areas (boxes on Figure 1) the rate is significantly higher than average, while in others it is lower. Studying variability of the association rates is a multivariate analysis, in which new information will affect the a priori distribution for each variable, which will in turn modify the induced event probability. Additional factors that may affect the likelihood of induced seismicity include variables expressing the geologic setting, poroelastic properties, and so on. As an example, *Schultz et al.* [2016] noted that confirmed cases of induced earthquakes in central Alberta are focused in a narrow band along the margins of the Swan Hills Formation. They conjectured that the association is likely due to (1) reef nucleation preference for faulted basement areas and/or (2) enhanced permeability/porosity from diagenesis.

Figure 2a shows the outlines of the Swan Hills Formation [*Wendte and Uyeno*, 2005] and the location of hit cells in the central WCSB. The spatial error for the reef outlines was assessed as 10 km, but this is dependent on the density of wells used in the region, so it varies spatially. We calculate the shortest distance between both hit cells and miss cells (active cells not meeting the hit criteria) and the outline of the reefs. We utilize the outermost outline of the reefs to capture to first order the connection to the reef. This outline expresses where the reef nucleated so it is most likely to be influenced by the underlying structure. Subsequent deposited reef layers grew with changing conditions of the Devonian sea, so the role that basement influence played in their deposition becomes more ambiguous.

The hit rate for the selected region shown in Figure 2a, which is just the region that encompasses the reef outlines, is $R_{h10} = N_{\mathrm{Hit}}/N_{\mathrm{Active}} = 32/673 = 0.048$. This is higher than the upper range of the regional hit rate calculated considering the whole study area, suggesting that proximity to the reefs results in a greater likelihood

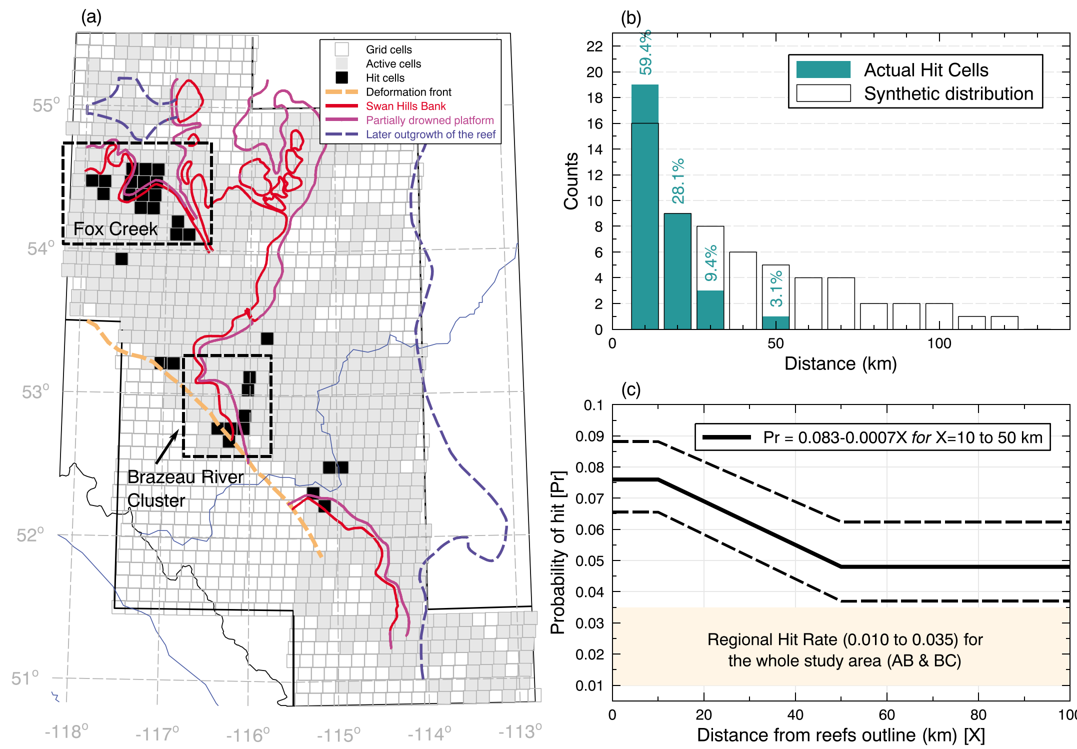

Figure 2. (a) The location of hit cells in comparison to the Swan Hills Formation outline in the central WCSB. The dashed black areas show the Fox Creek and Brazeau River Clusters. (b) Distributions of closest distance to the reef outline for hit cells; the numbers represent the counts in actual hit cells as % of total; (c) model of the probability that of HF wells will be associated with $M \geq 3$ events as a function of distance from reef outlines. The solid line is the model describing the probability of being a hit cell as a function of distance from the reef outline; the dashed lines show uncertainty in the probability. The shaded area shows the regional hit rate for the study area as a whole (as shown in Figure 1).

of induced seismicity. Moreover, we note that the average distance of hit cells to reef outlines is only ~13 km. By contrast, the average distance of active cells to reef outlines (not considering whether they are hit cells or not) is much greater, ~52 km, when taken over the considered region. This suggests that the distance to the reef outline may be a significant predictive variable.

In Figure 2b, we show that ~60% of hit cells are within 10 km from the reef outline. As a check on significance, we generated 1000 synthetic catalogues of hit cells randomly distributed in space. The 95th percentile of counts of distances in each bin from 1000 synthetic catalogues are plotted in comparison to the observed distribution. We test the null hypothesis that the data in these two distributions are from the same continuous distribution, using the two-sample Kolmogorov-Smirnov test. The test rejects the null hypothesis at the 5% significance level with a p-value of 0.0076. This means that the observed relationship between hit cells and reef outline is very unlikely to be coincidental. Despite the fact that the adopted approaches in this study and *Schultz et al.* [2016] are very different (in both method and data set), the same conclusion is reached—the reef is having a measurable effect on the distribution of seismicity in this region.

The way in which distance to the reef outline could be considered in a hazard analysis is also shown in Figure 2c. If we have an active cell at the average distance of ~50 km from the reef outline, the probability of its being a hit is 0.048 (i.e., assuming that the average hit rate corresponds to the average reef distance). This probability increases by ~60% if we are within 10 km of the reef outline (i.e., $0.048 \times 1.60 = 0.0768$). Having these two values, we can construct a simple model to describe the probability of being a hit cell as a function of distance from the reef outline. This model is composed of line segments, with a constant probability inside 10 km(=0.0768), and a constant probability beyond 50 km(=regional probability, which can be considered to be the background hit rate). We consider the uncertainty for the hit rate in this model to be comparable to that for the regional hit rate for the study area as a whole. The reason the rates for the function are all higher than the regional hit rate is because the function applies to only a subset of the region. In this considered subset (the area that includes the reefs), the association rates are higher in general, even for sites >50 km from the reef outline. Also, note that we cannot claim that the probability dies to zero at large distances. The *Pr* function is a compound probability, and its interpretation is complicated because being close to reefs may increase the probability of a hit, but being far away does not impart any specific information on *Pr*.

We are impressed by the strong apparent association between reef formations and the observed seismicity in central Alberta, but caution that this association may not necessarily be generalized to the other regions. We stress that the reef formation indicator is simply a prior estimate of proximity to basement controlled faults but is not entirely diagnostic of its presence or absence. There remains some likelihood for the presence of basement faults, most of which are unknown, for any cell. Possibly, other markers for such faults could also exist. For example, hydrothermal dolomite could be another important geological marker, as it suggests not just the presence of faults but also the potential for hydraulic communication with basement [see *Schultz et al.*, 2016].

There are a number of possible additional markers that could be considered in the attempt to refine the a priori distributions of likelihood of association of HF operations with seismicity. Often, models of induced seismicity invoke preexisting faults, which are both critically stressed and favorably oriented [*Reiter et al.*, 2014]. The lack of data for high-resolution structural-geology interpretations is a limiting factor to definitively determine if any faults are in a critical state in WCSB. Nevertheless, from focal mechanism and in situ stress considerations, one can make some inferences based on the current tectonic stress regime. It may be feasible to construct probabilistically framed arguments based on such considerations, which could be updated as new information on fault systems and states becomes available.

Another factor to consider further is the presence of nearby disposal wells, which may increase pore pressures in the subsurface, promoting the subsequent triggering of induced events by the small additional kick provided by HF operations. Further investigation of the combined effects of HF operations and disposal wells on the subsurface is needed to develop a model based on the apparent associations noted in this study.

Earthquake triggering by transient stresses from the seismic waves of distant main shocks has been documented in many studies [*Hill et al.*, 1993; *Gomberg et al.*, 2001; *Prejean et al.*, 2004; *Brodsky and van der Elst*, 2014]. Triggering propensity may be correlated with conditions such as volcanic or geothermal activity and extensional tectonics [*Brodsky and Prejean*, 2005; *Moran et al.*, 2004; *Harrington and Brodsky*, 2006]. Most cases of observed remote dynamic triggering are where natural earthquakes tend to occur, but recent studies show triggering in regions with low levels of historical seismicity, including the WCSB [*Wang et al.*, 2015]. Locations where triggering occurs may therefore reveal regions of critical ambient stress conditions, independent of proximity to plate boundary faults [*van der Elst et al.*, 2013]. A comprehensive catalogue of smaller events is required to detect and resolve faults in a region by means of remotely triggered seismicity. However, this may also be a promising avenue for constructing probabilistic indicators of the likelihood of future induced events.

7. Conclusions

In this study we developed a preliminary statistical model for induced seismicity. The calculated hit rate ratio gives us the regional probability that operations in a cell of 10 km radius may induce seismicity; this provides an estimate of the prior probability of inducing seismicity by commencing operations in a small area. Our main conclusions are as follows.

1. For the geological setting and operational parameters in the WCSB, the likelihood that hydraulic fracture operations in an area of 10 km radius will be associated with $M \geq 3$ earthquakes is 0.010 to 0.026, at the 95th percentile confidence limit. This is the likelihood averaged over the entire region. In some areas the rate is significantly higher than average, while in others it is lower.
2. The proximity of a nearby disposal well increases the likelihood that HF operations will be associated with seismicity.
3. Proximity to the Swan Hills Formation (a proxy for likely existence of basement controlled faults) is associated with increased seismogenic potential of HF operations. Specifically, the hit rate is higher for cells within 10–20 km of the reef edge as denoted by the Swan Hills Formation.

Acknowledgments
This work is supported by a collaborative development project funded by the Natural Sciences and Engineering Research Council of Canada, TransAlta, and Nanometrics. The database of ~700,000 wells (all types) from 1985 to 31/8/2015, as obtained from the Alberta Energy Regulator and the B.C. Oil and Gas Commission, was searched by using geoSCOUT software (geologic systems Ltd.) licensed to Western University. Western University thanks geoLOGIC Systems, Ltd., for the donation of geoSCOUT software licenses. The earthquake database is available at www.inducedseismicity.ca. Earthquake catalog simulations were performed by using the EQHAZ1 algorithm of *Assatourians and Atkinson* [2013], available at www.seismotoolbox.ca. We thank the Associate Editor (Andrew Newman), Ryan Schultz, and an anonymous reviewer for constructive comments that led to improvements in the manuscript.

References

Adams, J., and S. Halchuk (2003), Fourth generation seismic hazard maps of Canada: Values for over 650 Canadian localities intended for the 2005 National Building Code of Canada, *Geol. Surv. Canada Open File Rep., 4459*, 150 pp.

Assatourians, K., and G. M. Atkinson (2013), EqHaz: An open-source probabilistic seismic-hazard code based on the Monte Carlo simulation approach, *Seismol. Res. Lett.*, *84*, 516–524.

Atkinson, G. (2015), Ground-motion prediction equation for small-to-moderate events at short hypocentral distances, with application to induced seismicity hazards, *Bull. Seismol. Soc. Am.*, *105*(2A), 981–992.

Atkinson, G., B. Worden, and D. Wald (2014), Intensity prediction equations for North America, *Bull. Seismol. Soc. Am.*, *104*, 3084–3093.

Atkinson, G., K. Assatourians, B. Cheadle, and W. Greig (2015a), Ground motions from three recent earthquakes in western Alberta and northeastern British Columbia and their implications for induced-seismicity hazard in eastern regions, *Seismol. Res. Lett.*, *86*, 1022–1031.

Atkinson, G. M., H. Ghofrani, and K. Assatourians (2015b), Impact of induced seismicity on the evaluation of seismic hazard: Some preliminary considerations, *Seismol. Res. Lett.*, *86*, 1009–1021.

Atkinson, G. M., et al. (2016), Hydraulic fracturing drives induced seismicity in the Western Canada Sedimentary Basin, *Seismol. Res. Lett.*, *87*(3), 631–647.

B.C. Oil and Gas Commission (2012), Investigation of observed seismicity in the Horn River Basin. [Available at https://www.bcogc.ca/node/8046/download, (accessed 1 June 2016).]

B.C. Oil and Gas Commission (2014), Investigation of observed seismicity in the Montney Trend. [Available at https://www.bcogc.ca/node/12291/download, (accessed 1 June 2016).]

Brodsky, E. E., and S. G. Prejean (2005), New constraints on mechanisms of remotely triggered seismicity at Long Valley Caldera, *J. Geophys. Res.*, *110*, B04302, doi:10.1029/2004JB003211.

Brodsky, E. E., and N. J. van der Elst (2014), The uses of dynamic earthquake triggering, *Annu. Rev. Earth Planet. Sci.*, *42*(42), 317–339, doi:10.1146/Annurev-Earth-060313-054648.

Choi, C. (2012), Fracking earthquakes: Injection practice linked to scores of tremors, LiveScience, August, 6. Retrieved from. [Available at http://www.livescience.com/22151-fracking-earthquakes-fluidinjection.html.]

Ellsworth, W. L. (2013), Injection-induced earthquakes, *Science*, *341*(6142), Retrieved from http://www.sciencemag.org/content/341/6142/1225942.full, (accessed 1 June 2016).

Farahbod, A., H. Kao, J. Cassidy, and D. Walker (2015), How did hydraulic-fracturing operations in the Horn River Basin change seismicity patterns in northeastern British Columbia, Canada?, *Leading Edge*, *34*, 658–663.

Frankel, A. (1995), Mapping seismic hazard in the central and eastern United States, *Seismol. Res. Lett.*, *66*(4), 8–21.

Frohlich, C., W. Ellsworth, W. Brown, M. Brunt, J. Luetgert, T. MacDonald, and S. Walter (2014), The 17 May 2012 M4.8 earthquake near Timpson, East Texas: An event possibly triggered by fluid injection, *J. Geophys. Res. Solid Earth*, *119*, 581–593, doi:10.1002/2013JB010755.

Gomberg, J., P. A. Reasenberg, P. Bodin, and R. A. Harris (2001), Earthquake triggering by seismic waves following the Landers and Hector Mine earthquakes, *Nature*, *411*(6836), 462–466, doi:10.1038/35078053.

Hainzl, S., and Y. Ogata (2005), Detecting fluid signals in seismicity data through statistical earthquake modeling, *J. Geophys. Res.*, *110*, B05S07, doi:10.1029/2004JB003247.

Harrington, R. M., and E. E. Brodsky (2006), The absence of remotely triggered seismicity in Japan, *Bull. Seismol. Soc. Am.*, *96*(3), 871–878, doi:10.1785/0120050076.

Hill, D. P., et al. (1993), Seismicity remotely triggered by the magnitude 7.3 Landers, California, earthquake, *Science*, *260*(5114), 1617–1623, doi:10.1126/science.260.5114.1617.

Hornbach, M., et al. (2015), Causal factors for seismicity near Azle, Texas, *Nat. Commun.*, *6*, 6728, doi:10.1038/ncomms7728.

Keranen, K., M. Weingarten, G. Abers, B. Bekins, and S. Ge (2014), Sharp increase in central Oklahoma seismicity since 2008 induced by massive wastewater injection, *Science*, *345*, 448–451.

Moran, S. C., J. A. Power, S. D. Stihler, J. J. Sanchez, and J. Caplan-Auerbach (2004), Earthquake triggering at Alaskan volcanoes following the 3 November 2002 Denali fault earthquake, *Bull. Seismol. Soc. Am.*, *94*(6B), S300–S309.

National Research Council (2013), *Induced Seismicity Potential in Energy Technologies*, National Academies Press, Washington, D. C.

Prejean, S., D. Hill, E. E. Brodsky, S. Hough, M. Johnston, S. Malone, D. Oppenheimer, A. Pitt, and K. Richards-Dinger (2004), Remotely triggered seismicity on the United States west coast following the Mw 7.9 Denali Fault earthquake, *Bull. Seismol. Soc. Am.*, *94*(6B), S348–S359.

Reiter, K., O. Heidbach, D. Schmitt, K. Haug, M. Ziegler, and I. Moeck (2014), A revised crustal stress orientation database for Canada, *Tectonophysics*, *636*(1), 111–124.

Rubinstein, J., and A. Babaie Mahani (2015), Myths and facts on wastewater injection, hydraulic fracturing, enhanced oil recovery, and induced seismicity, *Seismol. Res. Lett.*, *86*(4), 1060–1067.

Schultz, R., S. Mei, D. Pana, V. Stern, Y. Gu, A. Kim, and D. Eaton (2015a), The Cardston earthquake swarm and hydraulic fracturing of the "Alberta Bakken" play, *Bull. Seismol. Soc. Am.*, *105*(6), 2871–2884.

Schultz, R., V. Stern, Y. Gu, and D. Eaton (2015b), Detection threshold and location resolution of the Alberta Geological Survey Earthquake Catalogue, *Seismol. Res. Lett.*, *86*(2A), 385–397.

Schultz, R., V. Stern, M. Novakovic, G. Atkinson, and Y. Gu (2015c), Hydraulic fracturing and the Crooked Lake Sequences: Insights gleaned from regional seismic networks, *Geophys. Res. Lett.*, *42*, 2750–2758, doi:10.1002/2015GL063455.

Schultz, R., H. Corlett, K. Haug, K. Kocon, K. MacCormack, V. Stern, and T. Shipman (2016), Linking fossil reefs with earthquakes: Geologic insight to where induced seismicity occurs in Alberta, *Geophys. Res. Lett.*, *43*, 2534–2542, doi:10.1002/2015GL067514.

Shapiro, S. A., E. Huenges, and G. Borm (1997), Estimating the crust permeability from fluid-injection-induced seismic emission at the KTB site, *Geophys. J. Int.*, *131*, F15–F18.

Taylor, O., A. Lester, and T. Lee (2015), Unconventional hydrocarbon development hazards within the central United States, U.S. Army Corps of Engineers, Engineer Research and Development Center Report, ERDC/GSL TR-15-26.

van der Elst, N. J., H. M. Savage, K. M. Keranen, and G. A. Abers (2013), Enhanced remote earthquake triggering at fluid-injection sites in the midwestern United States, *Science*, *341*(6142), 164–167, doi:10.1126/science.1238948.

Wang, B., R. M. Harrington, Y. Liu, H. Yu, A. Carey, and N. J. Elst (2015), Isolated cases of remote dynamic triggering in Canada detected using cataloged earthquakes combined with a matched-filter approach, *Geophys. Res. Lett.*, *42*, 5187–5196, doi:10.1002/2015GL064377.

Weingarten, M., S. Ge, J. W. Godt, B. A. Bekins, and J. L. Rubinstein (2015), High-rate injection is associated with the increase in U.S. mid-continent seismicity, *Science*, *348*(6241), 1336–1340.

Wendte, J. C., and T. Uyeno (2005), Sequence stratigraphy and evolution of Middle to Upper Devonian Beaverhill Lake strata, south-central Alberta, *Bull. Can. Petrol. Geol.*, *53*, 250–354.

Zoback, M., (2012), Managing the seismic risk posed by wastewater disposal, Earth, American Geological Institute. [Available at http://www.earthmagazine.org/article/managing-seismic-risk-posed-wastewater-disposal, (accessed 23 May 2016).]